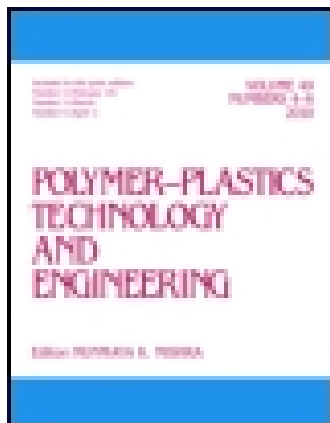


This article was downloaded by: [Cochin University of Science & Technology]

On: 31 July 2014, At: 21:28

Publisher: Taylor & Francis

Informa Ltd Registered in England and Wales Registered Number: 1072954 Registered office: Mortimer House, 37-41 Mortimer Street, London W1T 3JH, UK



## Polymer-Plastics Technology and Engineering

Publication details, including instructions for authors and subscription information:

<http://www.tandfonline.com/loi/lpte20>

### Physicomechanical and Magnetic Properties of Neoprene Based Rubber Ferrite Composites

K. H. Prema<sup>a</sup>, Philip Kurian<sup>b</sup>, P. A. Joy<sup>c</sup> & M. R. Anantharaman<sup>d</sup>

<sup>a</sup> Department of Polymer Science and Rubber Technology, Cochin University of Science and Technology, Cochin, India; S. D. College, Alappuzha-688 033, India

<sup>b</sup> Department of Polymer Science and Rubber Technology, Cochin University of Science and Technology, Cochin-682 022, India

<sup>c</sup> Physical Chemistry Division, National Chemical Laboratory, Pune-411 008, India

<sup>d</sup> Department of Physics, Cochin University of Science and Technology, Cochin-682 022, India

Published online: 30 Jan 2008.

To cite this article: K. H. Prema, Philip Kurian, P. A. Joy & M. R. Anantharaman (2008) Physicomechanical and Magnetic Properties of Neoprene Based Rubber Ferrite Composites, Polymer-Plastics Technology and Engineering, 47:2, 137-146, DOI: [10.1080/03602550701815946](https://doi.org/10.1080/03602550701815946)

To link to this article: <http://dx.doi.org/10.1080/03602550701815946>

PLEASE SCROLL DOWN FOR ARTICLE

Taylor & Francis makes every effort to ensure the accuracy of all the information (the "Content") contained in the publications on our platform. However, Taylor & Francis, our agents, and our licensors make no representations or warranties whatsoever as to the accuracy, completeness, or suitability for any purpose of the Content. Any opinions and views expressed in this publication are the opinions and views of the authors, and are not the views of or endorsed by Taylor & Francis. The accuracy of the Content should not be relied upon and should be independently verified with primary sources of information. Taylor and Francis shall not be liable for any losses, actions, claims, proceedings, demands, costs, expenses, damages, and other liabilities whatsoever or howsoever caused arising directly or indirectly in connection with, in relation to or arising out of the use of the Content.

This article may be used for research, teaching, and private study purposes. Any substantial or systematic reproduction, redistribution, reselling, loan, sub-licensing, systematic supply, or distribution in any form to anyone is expressly forbidden. Terms & Conditions of access and use can be found at <http://www.tandfonline.com/page/terms-and-conditions>

# Physicomechanical and Magnetic Properties of Neoprene Based Rubber Ferrite Composites

K. H. Prema<sup>1</sup>, Philip Kurian<sup>2</sup>, P. A. Joy<sup>3</sup>, and M. R. Anantharaman<sup>4</sup>

<sup>1</sup>Department of Polymer Science and Rubber Technology, Cochin University of Science and Technology, Cochin, India; S. D. College, Alappuzha–688 033, India

<sup>2</sup>Department of Polymer Science and Rubber Technology, Cochin University of Science and Technology, Cochin–682 022, India

<sup>3</sup>Physical Chemistry Division, National Chemical Laboratory, Pune–411 008, India

<sup>4</sup>Department of Physics, Cochin University of Science and Technology, Cochin–682 022, India

---

Fine (approximately 18 nm) particles of nickel ferrite were synthesized by the sol-gel technique, and their structural properties were evaluated by X-ray diffraction. Neoprene-based rubber ferrite composites were prepared by incorporating these nickel ferrite powders in the rubber matrix according to a specific recipe. The cure characteristics were analyzed, and the samples were molded into particular shapes whose properties were determined according to ASTM standards. Magnetization studies were carried out using a Vibrating Sample Magnetometer. This study indicates that neoprene rubber-based flexible magnets with desired magnetic properties and appropriate mechanical properties can be prepared by incorporating an adequate amount of nanoscale nickel ferrite particles within the rubber matrix.

---

**Keywords** Ferrite; Flexible magnets; Neoprene rubber; Rubber ferrite composites; Sol-gel method

## INTRODUCTION

Composite materials have many advantages over monolithic materials, because their mechanical properties can be tailored for particular applications. Rubber ferrite composites are one such class of composite materials, and their matrix properties can be modified to tailor their magnetic and dielectric properties. Incorporation of ferrites in an elastomer matrix produces rubber ferrite composites (RFCs)<sup>[1–6]</sup>. The difficulty of processing and molding ceramic magnetic materials into any shapes desired is their major disadvantage. Flexible magnets having superior processability and moldability can be prepared by incorporating ceramic magnetic materials within a flexible matrix, such as rubber<sup>[7]</sup>.

Particulate-filled rubber composites are commercially significant materials, and the mechanism of reinforcing the polymer matrix with fillers is important in the manufacture of polymer products. Very fine particle fillers, such as silicon carbide, calcium carbonate, silicates, and carbon black, are the most commonly used reinforcers<sup>[8–10]</sup>. Factors influencing the reinforcement of particulate fillers in an elastomer matrix include particle size and surface area and filler surface activity<sup>[11]</sup>. Surface area controls polymer–filler interaction in the composites, and surface activity controls filler–filler and filler–polymer interactions.

Fine particles of ferrite fillers impart characteristic magnetic and dielectric properties to an elastomer matrix, enhancing a composite's mechanical properties. Investigations into the effect of magnetic fillers on the physicomechanical properties of elastomers seldom occur. The present study investigates both the reinforcing characteristics of nickel ferrite nanoparticles in neoprene rubber and their effect on cure, mechanical, and magnetic properties of the RFCs.

RFCs are used in a wide variety of devices, including EMI shields and microwave absorbers<sup>[12,13]</sup>. RFCs with appropriate saturation magnetization values can be prepared by selecting an appropriate ferrite as the filler. Solomon, et al have reported that when ferrite fillers were incorporated into an elastomer, magnetic properties are imparted to the elastomer, its mechanical properties are improved, and the dielectric behavior of the matrix is modified<sup>[14]</sup>.

Ferrites are one of the most important classes of magnetic filler and can be classified into soft and hard ferrites. Nickel ferrite (NiO-Fe<sub>2</sub>O<sub>3</sub>) is a particularly important member of the ferrite family. It is a soft magnetic material having high saturation magnetization and low eddy currents<sup>[15]</sup>. Nickel ferrite crystallizes in an inverse spinel

---

Address correspondence to Philip Kurian. Tel.: 91 484 2575723; Fax: 91 484 2577747; E-mail: pkurian@cusat.ac.in

structure. The structure and saturation magnetization of ferrites depend on the grain size of a sample as well as upon its method of preparation. Several methods have been reported for the preparation of ferrites, such as the ceramic method<sup>[16]</sup>, coprecipitation<sup>[17]</sup>, and the sol-gel technique<sup>[18]</sup>. One of the easiest ways to synthesize nanosized particles is the sol-gel technique. This method has several advantages over conventional ceramic methods and is a cost-effective, low-temperature method for synthesizing nanosized particulate materials. In the present study, fine particles of NiFe<sub>2</sub>O<sub>4</sub> (Nif) were prepared using the sol-gel method, characterized, and incorporated into neoprene rubber.

Neoprene is a polar synthetic rubber having several resistant properties superior to natural rubber, including better resistance to gasoline, to weathering, to ozone, to oxidation, to flame, and to corrosive chemicals<sup>[19]</sup>.

RFCs were prepared by incorporating nickel ferrite in neoprene rubber according to a specific recipe. The cure characteristics and mechanical properties of these RFCs were studied and reported here.

The magnetic properties of the composites, such as the saturation magnetization, were measured and reported along with those of the filler. A mixture equation was used to calculate the theoretical saturation magnetization value of the composites from that of the nickel ferrite and the neoprene matrix<sup>[20]</sup>.

## EXPERIMENTAL

### Preparation of Nickel Ferrite

Nickel ferrite (Nif) was prepared by means of the sol-gel method<sup>[21]</sup> using analytical-grade nickel nitrate and ferric nitrate. Solutions of ferric nitrate and nickel nitrate in pure ethylene glycol were mixed in a 2:1 molar ratio and heated to 40°C. The gel thus obtained was then dried at 90°C, upon which it self-ignited, creating a fluffy, voluminous product. The samples were then homogenized by ball milling using a Fritsch Pulverisette ultrasonic grinder for twenty minutes and were then heated to 200°C for 2 hours to eliminate any volatile impurities.

### Characterization of Nickel Ferrite

The nickel ferrite powder prepared was characterized using an X-ray powder diffraction technique (Rigaku Dmax-C) with Cu K $\alpha$  radiations. The average particle size was then determined using the Debye-Scherrer formula

$$D = \frac{0.9\lambda}{\beta \cos \theta} \quad (1)$$

where D is the average particle size,  $\lambda$  is the wavelength,  $\beta$  is the full width at half maximum in radians, and  $\theta$  is the Bragg angle.

### Preparation of Neoprene Based RFCs

Precharacterized nickel ferrite powder was incorporated in the neoprene rubber (W grade) according to a specific recipe (Table 1). RFCs were prepared with nickel ferrite ranging from 40 phr to 120 phr in steps of 20. A control compound was prepared without any filler. Mixing was carried out in a Brabender Plasticorder, Model PL 3S, per ASTM D3182-89 (2001). The mixing was carried out at 60°C with a rotor speed of 50 rpm. The mixed stock was homogenized using a two-roll mill with a 0.8 mm nip gap and was then made into sheets 2.4 mm thick.

### Evaluation of Cure Characteristics

Cure characteristics of the RFCs were determined using a Rubber Processing Analyzer (RPA 2000 of  $\alpha$ -Technology) at a temperature of 160°C. From the RPA results, the optimum cure time ( $t_{90}$ ) and the scorch time ( $t_{10}$ ) were evaluated along with the maximum and minimum torque values.

### Preparation of Test Specimen

Rubber compounds were compression-molded into sheets about 2 mm thick using an electrically heated hydraulic press having 45 cm  $\times$  45 cm platens at a pressure of 140 kg/cm<sup>2</sup> in a standard mold. Rubber compounds were cured up to their respective cure times at 160°C. Dumbbell

TABLE 1  
Recipe used for the preparation of neoprene based RFCs

Material	CR0	CR40	CR60	CR80	CR100	CR120
Neoprene	100	100	100	100	100	100
MgO	4	4	4	4	4	4
Stearic acid	1	1	1	1	1	1
Nif (filler)	0	40	60	80	100	120
Naphthaneic oil	0	4	6	8	10	12
NA22	0.5	0.5	0.5	0.5	0.5	0.5
ZnO	5	5	5	5	5	5

specimens for the stress strain measurements were cut from the vulcanized sheet using an ASTM D-type die.

### Evaluation of Mechanical Properties

#### Stress–Strain Measurement

The stress–strain properties, such as tensile strength, modulus, and elongation at break, were determined using Shimadzu universal testing machine model SPL 10 KN at a cross head speed of 500 mm/min. Stress-strain measurements were carried out, per ASTM D 412-98a(2002).

#### Tear Strength

Tear resistance of the samples was tested, per ASTM D 624-2000, using test specimens having a 90° angle on one side and tab ends punched out from the molded sheets along the mill grain direction.

#### Hardness

Sample hardness was measured, per ASTM D 2240-03, using a Shore A Durometer and a sample 6 mm thick. Readings were taken after 15 seconds of pressure after firm contact was established with the specimens.

#### Resilience

Sample resilience was measured, per ASTM D 2632-2001, with a vertical rebound resiliometer, using cylindrical samples 16 mm in diameter and 6 mm thick.

#### Abrasion Resistance

Sample abrasion resistance was measured using a DIN abrader (DIN 53516), per ASTM D 5963-2001. Cylindrical samples 16 mm in diameter and 20 mm long were kept on a rotating sample holder, and a load of 10 N was applied. Weights of the samples before and after the run were taken, and the volume loss was estimated.

#### Cross-Link Density

The cross-link density (CLD) of vulcanized samples was determined by the equilibrium swelling method using the Florey–Rehner equation. Samples of approximately 0.3 g were accurately weighed and kept in toluene solvent in an airtight container for 24 hours. The outer portion of the swollen samples was then gently wiped with filter paper and weighed. The samples were again stored in solvent and weighed at intervals of 1 hour until an equilibrium weight was obtained. The swollen samples were heated at 60°C for 24 hours in an oven to remove the solvent. The de-swollen weight was then taken. The volume fraction of rubber in the de-swollen network was then calculated using the equation

$$V_r = \frac{(D - FT)\rho_r^{-1}}{(D - FT)\rho_r^{-1} + A_0\rho_s^{-1}} \quad (2)$$

where T is the weight of the test specimen, D is the specimen's de-swollen weight, F is the weight fraction of the insoluble component,  $A_0$  is the weight of the absorbed solvent, corrected for the swelling increment,  $\rho_r$  is the density of the test specimen, and  $\rho_s$  is the density of the solvent.

### Magnetic Measurements

The magnetic parameters of the nickel ferrite and the RFCs were measured at room temperature using a Vibrating Sample Magnetometer (model EG&G PAR 4500). A hysteresis loop was plotted, and parameters such as saturation magnetization ( $M_s$ ), coercivity ( $H_c$ ), and magnetic remanence were evaluated.

### Morphology

The morphological characterization of the fractured surfaces of the tensile test specimens was carried out using a Scanning Electron Microscope (Cambridge Instruments S 360 stereo scanner version VO2-01) and the scanning electron micrographs were recorded. Gold was spattered on the samples before they were scanned.

## RESULTS AND DISCUSSION

### Structural Characterization of NiFe<sub>2</sub>O<sub>4</sub>

The X-ray diffraction pattern of nickel ferrite powder is depicted in Figure 1. All the characteristic peaks of nickel ferrite are present in the diffraction diagram. The powder diffraction pattern agrees well with the JCPDS values (JCPDS No. 74-2081)<sup>[22]</sup>. The average particle size, calculated by means of the Debye–Scherrer equation, is 19 nm. The lattice parameter 'a' is calculated to be 8.328 Å. The slightly broad pattern of XRD was caused by the smaller grain size of the ferrite particles.

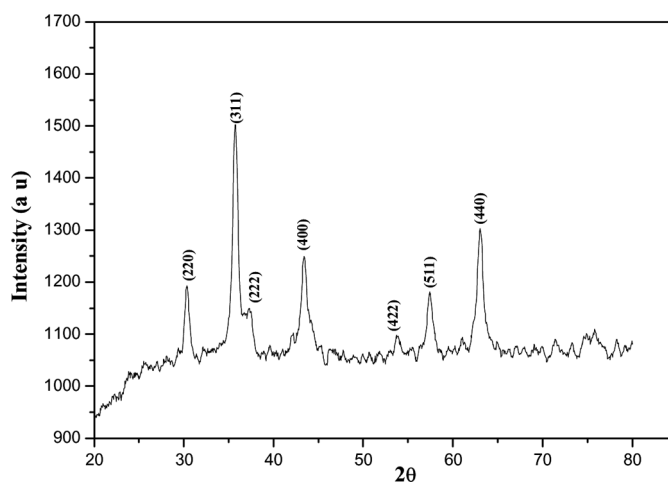


FIG. 1. X-ray diffraction of NiFe<sub>2</sub>O<sub>4</sub>.

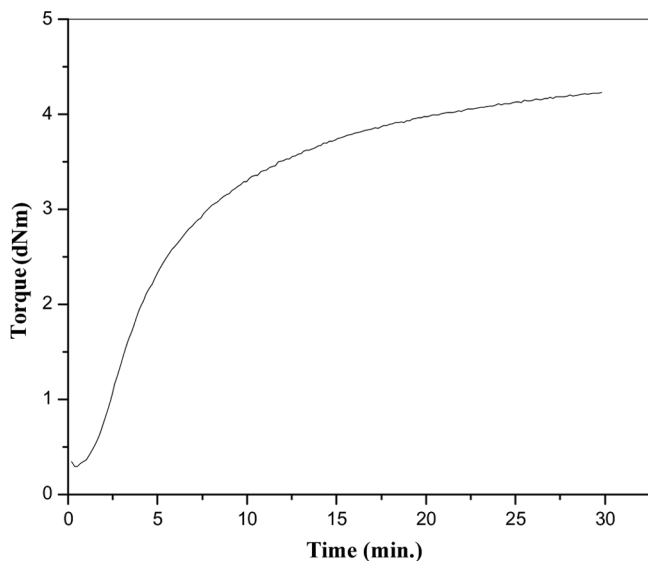


FIG. 2. Representative cure curve for RFCs.

### Cure Characterization of RFCs

The cure characteristics of the prepared RFCs were determined using a rubber processing analyzer (RPA 2000 of  $\alpha$ -Technology). A typical cure curve of the rubber ferrite composite is shown in Figure 2.

The variation in maximum torque ( $D_{\max}$ ) and minimum torque ( $D_{\min}$ ) of the loaded nickel ferrite are shown in Table 2. Maximum torque indicates the shear modulus of the fully vulcanized rubber at vulcanization temperature. Maximum torque increases markedly with Nif. Because the shear force is higher at the time of mixing, the elastomer breaks down and active sites are created that then combine with nanosized filler particles to increase the shear modulus of the RFCs, demonstrating the reinforcing nature of the ferrite filler.

The variation in minimum torque of the loaded nickel ferrite is also given in Table 2. Minimum torque increases with ferrite filler loading. Minimum torque is a measure of the compound's viscosity. Even though the minimum torque increases with loading of ferrite filler, it does not

detract from the processability of the compound. Increase in viscosity with the addition of nickel ferrite is caused by the occlusion of rubber within and between the filler aggregates and as well as the immobilization of a layer of elastomer at the surface of the filler.

Wolf and Westlinning proposed a mathematical expression in terms of rheometric data, which give an idea about the bound structure of fillers in the vulcanizate, especially regarding carbon black-filled composites<sup>[23,24]</sup>. The ratio in the torque variance between loaded and unloaded compounds was found to be directly proportional to the filler loading. By plotting the relative torque against the fraction of filler loading, a straight line is obtained whose slope is defined by Wolf as  $\alpha_F$ <sup>[8,9]</sup>

$$\frac{D_{\max} - D_{\min}}{D_{\max}^0 - D_{\min}^0} - 1 = \alpha_F \frac{m_f}{m_p} \quad (3)$$

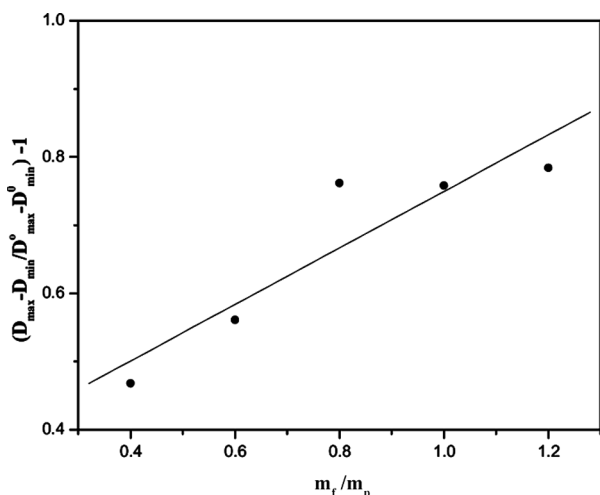
where  $m_f$  and  $m_p$  are the masses of filler and polymer in the compound and  $\alpha_F$  is a specific constant for the filler that gives an idea of the filler's final structure in the vulcanizate.

Figure 3a shows the plot of  $\frac{D_{\max} - D_{\min}}{D_{\max}^0 - D_{\min}^0} - 1$  against  $m_f/m_p$ . The nonlinear relationship of the relative torque to the filler loading indicates that the incorporation of nickel ferrite particles affects cross-linking between polymer chains. Cross-link density of the RFCs is given in Table 3. As the filler loading increases, the cross-link density decreases—a clear indication of filler-matrix interaction.

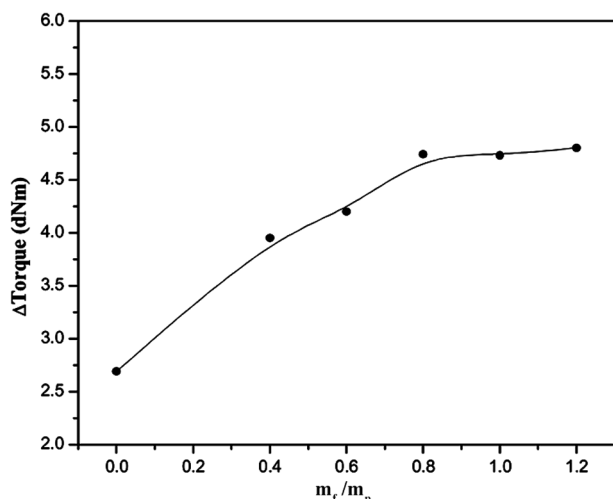
Figure 3b shows the plot of  $\Delta$  torque against filler loading.  $\Delta$  torque ( $D_{\max} - D_{\min}$ ) increases with filler loading initially, but, at higher loading levels, deviation from linearity is evident. At lower filler concentrations, the distance between filler particles is high and the rubber chains are attached to single filler particles, which causes the formation of a gel-like structure that is uniformly dispersed throughout the compound, resulting in a linear increase in  $\Delta$  torque. As the filler loading increases, the filler-filler distance decreases. At this stage, interparticular attachment of polymer chains occurs. The segmental mobility of the chain decreases further, and a coherent gel-type structure is formed. As a result,  $\Delta$  torque deviates from linearity at higher loading levels.

TABLE 2  
Cure characteristics of RFCs

Loading (phr)	Maximum torque (dNm)	Minimum torque (dNm)	Cure time $t_{90}$ (min)	Scorch time $t_{10}$ (min)	$ts_2$ (min)	CRI ( $\text{min}^{-1}$ )
0	2.98	0.29	12.75	1.01	7.02	17.49
40	4.24	0.29	16.97	1.86	4.87	8.26
60	4.48	0.28	16.99	2.28	5.39	8.62
80	5.08	0.34	17.51	2.34	3.82	7.304
100	5.12	0.39	20.03	2.49	6.22	7.24
120	5.27	0.47	23.29	2.76	8.49	6.76



(a)



(b)

FIG. 3. (a) Plot of  $\frac{D_{max} - D_{min}}{D_{max} - D_{min}} - 1$  against  $m_f/m_p$ ; (b) Relative torque against filler loading.

$\alpha_F$  for each composite is calculated using Equation 3; the variation in  $\alpha_F$  with filler loading is depicted in Figure 4. Higher values of  $\alpha_F$  indicate stronger filler–filler

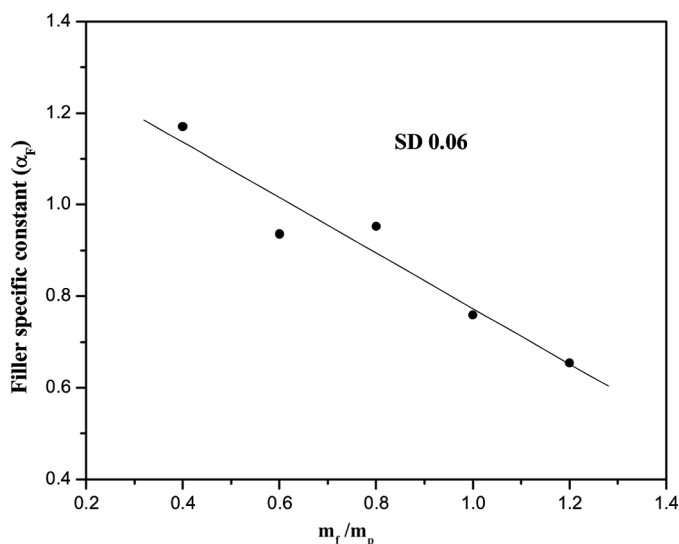


FIG. 4. Plot of  $\alpha$  against  $m_f/m_p$ .

interactions, which may result in the formation of a filler network at higher filler loadings. In Figure 4 it is evident that the value of  $\alpha_F$  decreases with nickel ferrite loading in neoprene rubber, indicating that even at higher loadings, ferrite does not form network structures in the neoprene matrix.

Table 2 demonstrates that cure time increases with filler loading as curatives are adsorbed over the active surfaces of the ferrite particles, lessening their concentration and increasing the time required for an optimum cure. These observations are further supported from the cure rate index values given in Table 2. The cure rate index (CRI) is a measure of the rate of the curing reaction and is given by the equation

$$CRI = \frac{100}{t_{90} - t_{s2}} \quad (4)$$

where  $t_{90}$  and  $t_{s2}$ , respectively, are the optimum cure time and the time required for two units' rise from the minimum torque value. With the incorporation of 20 phr Nif, the CRI value decreases by half to that of the gum vulcanizate.

TABLE 3  
Mechanical properties of RFCs

Loading (phr)	Tensile strength (MPa)	Elongation at break (%)	300% modulus (MPa)	Tear strength (N/mm)	Cross-link density (CLD) $10^{-5}$
0	13.99	1165	1.79	35.16	5.43
40	19.19	1290	2.07	35.55	4.36
60	18.59	1218	2.34	39.26	4.08
80	17.76	1194	2.53	36.69	3.78
100	15.59	1143	2.63	40.28	3.44
120	13.52	1092	2.72	41.5	3.98

The decrease in CRI value is caused by the wetting of the surface of the filler particles by the elastomer, which tends to intervene in the cross-linking reaction. But further additions of nickel ferrite cause only marginal decreases in CRI values.

Variations in the scorch time with the loading levels of ferrite filler are given in Table 2. The scorch time of the compound increases slightly with filler loading, indicating that the processability of the composite is not affected by the incorporation of nickel ferrite. This increase is caused by the adsorption of curatives over the surface of the ferrite particles.

## Mechanical Properties of RFCs

### Stress–Strain properties

Stress–strain properties, such as tensile strength, elongation at break, and modulus at 300% elongation, were measured and the values recorded in Table 3. The tensile strength of the RFCs was higher than that of the gum vulcanizate. A maximum tensile strength value of 19.19 MPa was obtained for 40 phr loading of ferrite filler. The tensile strength decreases at higher loadings of Nif. Tensile strength of the RFC with 120 phr of Nif is almost equal to that of gum vulcanizate. All this reveals the reinforcing nature of the ferrite particles in the neoprene rubber matrix. Both surface area and specific activity of the filler contribute to reinforcement—particle size physically, and surface activity chemically. The particle size of the synthesized nickel ferrite used for the preparation of the RFCs is about 18 nm. As their size decreases, the interface area between the filler and the elastomer increases, causing stronger reinforcement. As the loading increases above 40 phr, a regular decrease in tensile strength is evident. As the filler loading increases, the volume fraction of the rubber decreases, and sufficient wetting of the filler by the elastomer may not take place.

Elongation at break of the RFCs is given in Table 3, which shows the same trend exhibited by tensile strength. Because of the finer particle size of nickel ferrite, an improvement in the stress-bearing capacity of the polymer–filler interphase is observed at lower filler loadings. At higher loadings of ferrite fillers, elongation at break decreases because of poor interactions between the surface of the filler and rubber.

An increase in modulus at higher filler loadings is mainly caused by the inclusion of rigid filler particles in the soft matrix. Bridging of rubber chains between the filler particles enhances the modulus at 300% elongation.

### Tear Strength

Tear strength values of the RFCs are given in Table 3. As the filler loading increases, the tear strength of the

vulcanizate increases considerably, clearly exhibiting the reinforcing nature of Nif in a neoprene rubber matrix. In the filled neoprene rubber matrix, the filler interacts with the elastomer chains, creating a barrier to the tear path. Filler particles present at the propagation tip arrest the propagating cracks, increasing tear resistance<sup>[25]</sup>. Thus the tear strength of the RFCs increases with filler loading and is higher than the gum vulcanizate, even at 100 phr of nickel ferrite.

### Hardness

Figure 5 shows variations in hardness with ferrite loading. Hardness is a measure of the modulus at low levels of strain. Hardness of the RFCs increases with nickel ferrite loading because of the elastomer chains' decreased mobility.

### Resilience

Variations in the resilience of the neoprene rubber vulcanizate with the loading of nickel ferrite are given in Figure 5 and exhibit regular decreases with increases in filler content. Resilience is directly related to the rubber content of the vulcanizate. As the rubber content decreases, the damping characteristic of the compound decreases, decreasing resilience.

The decrease in rebound height with the increase of filler loading is linear, according to the equation

$$R_0 - R = A \frac{m_f}{m_p} \quad (5)$$

where  $R_0$  is the rebound height of the gum and  $R$  is that of the filled vulcanizate, and  $A$  is the filler-specific constant characteristic of the surface area of the filler available for interaction with rubber molecules. The plot of  $R_0 - R$  against  $m_f/m_p$  is given in Figure 6.

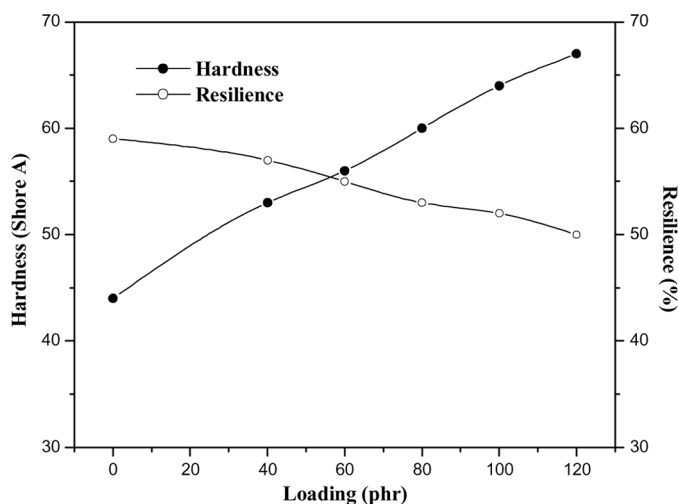


FIG. 5. Variation of hardness and resilience with filler loading.

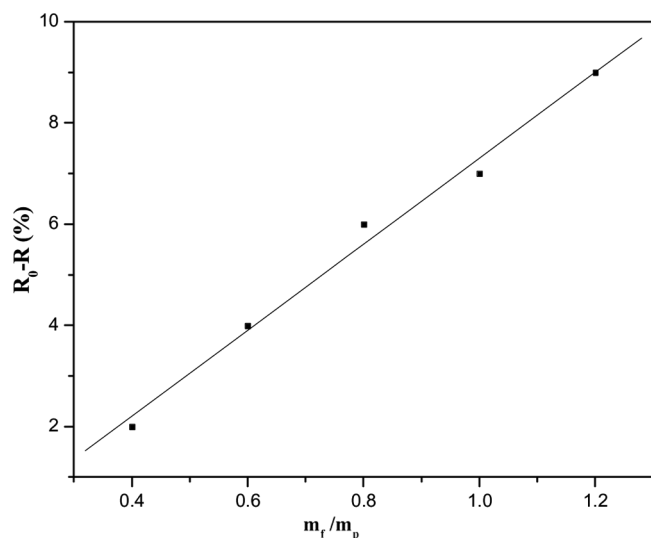


FIG. 6. Plot of  $R_0-R$  against  $m_f/m_p$ .

#### Abrasion Resistance

Volume loss caused by abrasion of the RFCs with loading of nickel ferrite is shown in Figure 7. As the neoprene rubber is loaded with Nif, the volume loss on abrasion decreases initially and then gradually increases. The abrasion resistance increases up to 60 phr loading of Nif and is caused by the smaller particle size of the ferrite filler. The interaction between the neoprene matrix and the filler restricts wear on the rubber during abrasion. At higher loadings of ferrite filler, the filler–filler interactions overcome the rubber–filler interactions, reducing abrasion resistance.

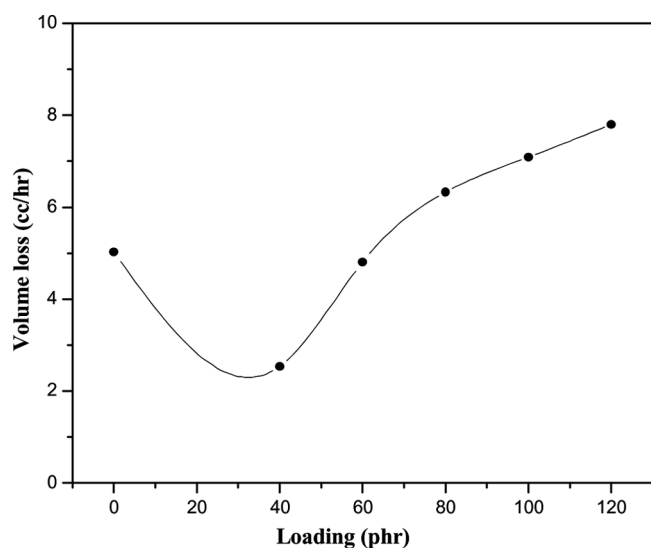


FIG. 7. Variation in volume loss on abrasion with filler loading.

#### Cross-Link Density

The cross-link densities (CLD) of the gum vulcanizate and of the RFCs are given in Table 3, where the greatest cross-link density is evident in the case of gum vulcanizate. As the nickel ferrite loading increases, the apparent CLD decreases as a result of the detachment of polymer from the polymer–filler interface and of the sorption of curatives on the filler surface<sup>[26]</sup>. This is supported by the morphology of the composites, recorded in the SEM photographs, which clearly show that as the nickel ferrite loading increases, filler agglomeration increases, reducing cross-link density.

#### Morphology

Scanning electron microscopic pictures of fractured surfaces in the gum vulcanizate and in the nickel ferrite containing RFCs are provided in Figure 8a–f. Figure 8a shows a smooth topography on the fractured surface of the gum vulcanizate, and Figure 8b–f shows the fractured surfaces of RFCs with 40, 60, 80, 100, and 120 phr of nickel ferrite, respectively. Figure 8b–f shows the even distribution of Nif in the neoprene matrix. Compared to the SEM image of the fractured surface of the gum vulcanizate, all other SEM show a rough topography that indicates a delay in the fracturing process. In the RFCs, at the initial stage of failure the stress distribution may be uniform; but, as failure intensifies, the stress distribution in the vulcanizate is nonuniform, resulting in a rough topography.

Voids present in the micrographs are the result of the detachment of filler aggregates from the rubber matrix. In Figure 8b,c, the average void size is approximately 3  $\mu\text{m}$ . A slight increase in void size can be seen at higher loading levels, caused by an increase in filler concentration that may lead to the formation of larger aggregates. Void size in Figure 8d is approximately 5  $\mu\text{m}$ ; the presence of a number of small additional voids can be observed, a result of the increased filler content on filler agglomeration. SEM pictures confirm the high tensile strength values of RFCs with 40, 60, and 80 phr of Nif, in which agglomeration of ferrite filler was found to be less than that of higher loadings.

#### Magnetic Measurements

The magnetic studies were carried out on the nickel ferrite and the rubber ferrite composites using a Vibrating Sample Magnetometer (VSM) determining the magnetic parameters—saturation magnetization ( $M_s$ ), coercivity ( $H_c$ ), and magnetic remanence. Figure 9 shows the hysteresis loop for the nickel ferrite filler and the hysteresis loops for the RFC with 120 phr nickel ferrite. The saturation magnetization and coercivity of the filler and composites were obtained from the corresponding hysteresis loops.  $M_s$  values

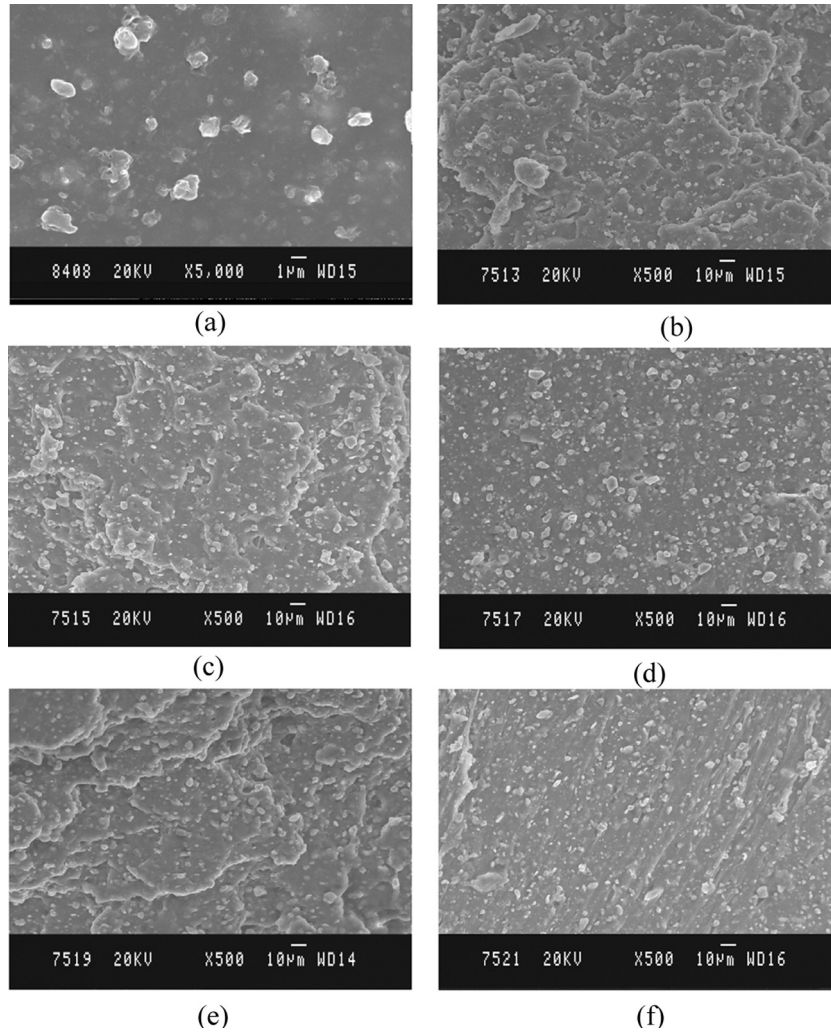


FIG. 8. (a) Scanning electron micrograph of tensile fractured surface of gum vulcanizate; (b) Scanning electron micrograph of tensile fractured surface of CR40; (c) Scanning electron micrograph of tensile fractured surface of CR60; (d) Scanning electron micrographs of tensile fractured surface of CR80; (e) Scanning electron micrographs of tensile fractured surface of CR100; (f) Scanning electron micrographs of tensile fractured surface of CR120.

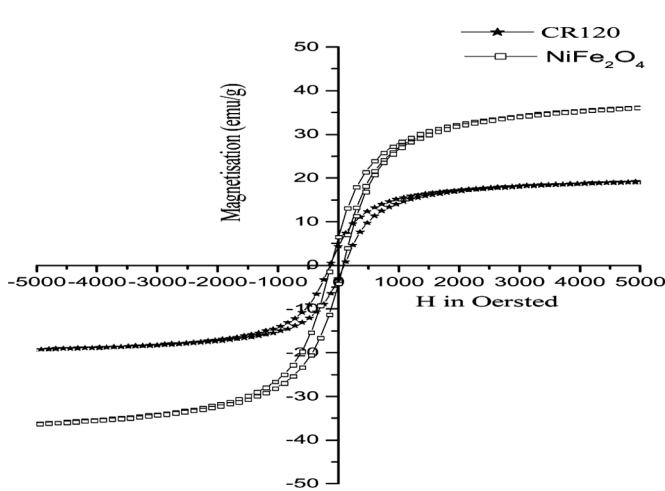


FIG. 9. Hysteresis loop for nickel ferrite filler and CR120.

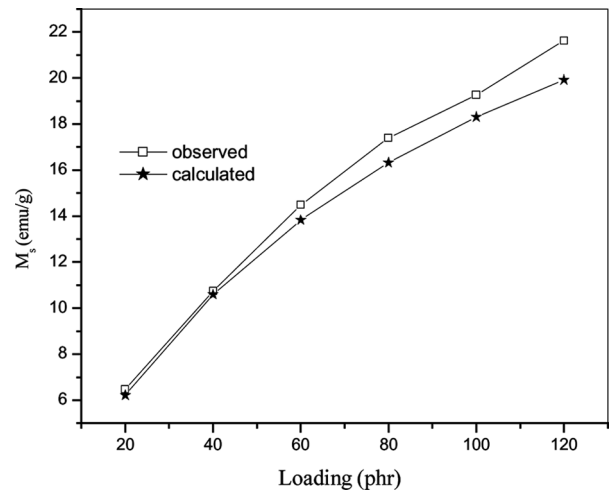


FIG. 10. Loading dependence of saturation magnetization.

TABLE 4  
Magnetic properties of RFCs and nickel ferrite

Nickel ferrite loading (phr)	Saturation magnetization (Ms)(emu/g)	Coercivity (Hc)(Oe)	Magnetic remanence (Mr)(emu/g)	Mr/Ms
40	10.47	115.25	2.21	0.21
60	14.01	115.25	2.79	0.20
80	16.73	115.25	3.53	0.21
100	18.82	115.42	3.65	0.19
120	20.72	115.42	3.83	0.18
Nickel ferrite	39.18	101.00	5.28	0.13

of the composites were found to depend on the loading of the filler, a discovery confirmed by the theoretical calculation of  $M_s$  values of the composites using the simple mixture equation

$$M_{\text{rfc}} = W_1 M_1 + W_2 M_2 \quad (6)$$

where  $W_1$  is the weight fraction of filler,  $M_1$  is the saturation magnetization of the filler,  $W_2$  is the weight fraction of the matrix, and  $M_2$  is the saturation magnetization of the matrix. Because the neoprene matrix is nonmagnetic, the Equation (6) can be reduced to

$$M_{\text{rfc}} = W_1 M_1 \quad (7)$$

The  $M_s$  values were calculated using Equation 7 and are shown in Figure 10.

The saturation magnetization value of Nif was 39.18, as obtained from the hysteresis loop. RFCs had different  $M_s$  values that depended on the amount of Nif. A maximum value of 20.72 was obtained in the case of 120 phr loading. The coercivity value of the nickel ferrite filler is 101 Oe. From Table 4 it can be observed that the coercivity value of all the RFCs is almost same—approximately 115 Oe—indicating that there is no chemical interaction between the filler and the rubber matrix. The small increase in  $H_c$  of RFCs from that of the Nif is attributable to the slight change in particle size of the filler during processing. Change in particle size of the filler within the matrix can be expected because the vulcanization took place at 160°C. RFCs with desired magnetic properties can be synthesized by incorporating appropriate amounts of nickel ferrite.

## CONCLUSION

Nickel ferrite was synthesized using the sol-gel method and characterized using an X-ray diffraction technique. Particles, which were cube-shaped, averaged 18 nm in size. Neoprene-based rubber ferrite composites were prepared with various loadings of nickel ferrite. The cure characteristics of the RFCs were evaluated using RPA. The cure time and scorch time of the RFCs increased with increases in the loading of nickel ferrite. Maximum and minimum torque values also increased with the increase of ferrite

loading in RFCs, and  $\alpha_F$  values for the vulcanizates decreased with increases in ferrite filler loading, indicating that neoprene rubber can accept high amounts of nickel ferrite filler with little agglomeration. Stress-strain properties of the RFCs, along with other mechanical properties, were also evaluated. RFCs with 40 phr of nickel ferrite showed the greatest tensile strength. RFCs with higher loadings of nickel ferrite showed tensile strength values higher than that of the gum vulcanizate. RFCs' elongations at break decreased with increases in ferrite loading. The tear strengths of all RFCs were higher than those of the gum vulcanizate. The resilience of the RFCs gradually decreased as hardness increased with the loading of nickel ferrite. The abrasion resistance of RFCs increased with increases in nickel ferrite loading up to 60 phr and then slightly decreased with higher loadings. The cross-link density of the RFCs was less than that of the gum vulcanizate. The saturation magnetization values of the RFCs depended on the loading of the ferrite filler.

## ACKNOWLEDGMENTS

P.K.H. thanks the University Grants Commission for the fellowship under the FIP scheme of the X plan period.

M.R.A. thanks the All India Council for Technical Education for the provision of ferrofluids. AICTE file No. 8023/RID/RPS-73/2004-05.

## REFERENCES

1. Yavuz, O.; Ram, M.K.; Aldissi, M.; Poddar, P.; Hariharan, S. Synthesis and the physical properties of MnZn ferrite and NiMnZn ferrite-polyaniline nanocomposite particles. *J. Mater. Chem.* **2005**, *15*, 810–817.
2. Sakamoto, R. Electrically-conductive rubbers with carbon black 3 electrically conductive rubber. *Intl. Polymer Sci. Tech.* **1987**, *14* (4), T/40–T/47.
3. Mohammed, E.M.; Malini, K.A.; Joy, P.A.; Kulkarni, S.D.; Date, S.K.; Kurian, P.; Anantharaman, M.R. Processability, hardness and magnetic properties of rubber ferrite composites containing manganese zinc ferrites. *Plas. Rub. Comp.* **2002**, *31* (3), 106–113.
4. Anantharaman, M.R.; Sindhu, S.; Jagathesan, S.; Malini, K.A.; Kurian, P. Dielectric properties of rubber ferrite composites containing mixed ferrites. *J. Phy. D. Appl. Phy.* **1999**, *32*, 1801–1810.

5. Annadurai, P.; Mallic, A.K.; Tripathy, D.K. Studies on microwave shielding materials based on ferrite and carbon black-filled EPDM rubber in the X-band. *J. App. Polymer Sci.* **2002**, *83*, 145–150.
6. Makled, M.H.; Matsui, T.; Tsuda, H.; Mabuchi, H.; El-Mansy, M.K.; Morii, K. Magnetic and dynamic mechanical properties of barium ferrite-natural rubber composites. *J. Mat. Proc. Tech.* **2005**, *160*, 229–233.
7. Marrett, C.; Moulart, A.; Colton, J. Flexible polymer composite electromagnetic crystals. *Polymer Eng. Sci.* **2003**, *43* (4), 822–830.
8. Kraus, G. Reinforcement of elastomers by carbon black. *Rub. Chem. Tech.* **1978**, *51* (1), 297–321.
9. Sobhy, M.S.; El-Nashar, D.E.; Maziad, N.A. Cure characteristics and physicomechanical properties of calcium carbonate reinforcement rubber composites. *Egypt. J. Sol.* **2003**, *26* (2), 241–257.
10. Kohjiya, S.; Ikeda, Y. Reinforcement of general-purpose grade rubbers by silica generated in situ. *Rub. Chem. Tech.* **2000**, *73* (3), 534–550.
11. Wolf, S.; Wang, M.-J. Filler-elastomer interactions. The effect of the surface energies of fillers on elastomer reinforcement. *Rub. Chem. Tech.* **1992**, *65* (2), 329–342.
12. Rigbi, Z.; Jilken, L. The response of an elastomer filled with soft ferrite to mechanical and magnetic influences. *J. Mag. Mag. Mat.* **1983**, *37*, 267–276.
13. Saini, D.R.; Shenoy, A.V.; Nadkarni, V.M. Dynamic mechanical properties of highly loaded ferrite filled thermoplastic elastomer. *J. App. Polymer Sci.* **1984**, *29* (12), 4123–4143.
14. Soloman, M.A.; Kurian, P.; Anantharaman, M.R.; Joy, P.A. Evaluation of the magnetic and mechanical properties of rubber ferrite composites containing strontium ferrite. *Polymer-Plastics Tech. Eng.* **2004**, *43* (4), 1013–1028.
15. Son, S.; Taheri, M.; Carpenter, E.; Harris, V.G.; McHenry, M.E. Synthesis of ferrite and nickel ferrite using radio-frequency thermal plasma torch. *J. App. Phys.* **2002**, *91* (10), 7589–7591.
16. Valenzuela, R. *Magnetic Ceramics*, 1st Ed., Cambridge University Press: New York, Chapter 3, 1994.
17. Shi, Y.; Ding, J.; Liu, X.; Wang, J. NiFe<sub>2</sub>O<sub>4</sub> ultrafine particles prepared by co-precipitation/mechanical alloying. *J. Mag. Mag. Mat.* **1999**, *205*, 249–254.
18. Silva, M.N.B.; dos S. Duque, J.G.; Gouveia, D.X.; de Paiva, J.A.C.; Macedo, M.A. Novel route for the preparation of nanosized NiFe<sub>2</sub>O<sub>4</sub> powders. *Jap. J. App. Phys.* **2004**, *43* (8A), 5249–5252.
19. Morton, M. *Rubber Technology*, 3rd Ed., Van Nostrand Reinold Company: New York, Chapter 12, 1995.
20. Malini, K.A.; Mohammed, E.M.; Sindhu, S.; Joy, P.A.; Date, S.K.; Kulkarni, S.D.; Kurian, P.; Anantharaman, M.R. Magnetic and processability studies on rubber ferrite composites based on natural rubber and mixed ferrite. *J. Mat. Sci.* **2001**, *36*, 5551–5557.
21. George, M.; John, A.M.; Nair, S.S.; Joy, P.A.; Anantharaman, M.R. Finite size effects on the structural and magnetic properties of sol-gel synthesized NiFe<sub>2</sub>O<sub>4</sub>. *J. Mag. Mag. Mat.* **2006**, *302*, 190–195.
22. Subramanyam, K.N. Neutron and X-ray diffraction studies of certain doped nickel ferrites. *J. Phys. C: Solid State Phys.* **1971**, *4*, 2266–2268.
23. da Costa, H.M.; Visconte, L.L.Y.; Nunes, R.C.R.; Furtado, C.R.G. Rice husk ash filled natural rubber compounds—the use of rheometric data to qualitatively estimate optimum filler loading. *Intl. J. Polym. Mat.* **2004**, *53*, 475–497.
24. Wolf, S. Chemical aspects of rubber reinforcement by fillers. *Rub. Chem. Tech.* **1996**, *69* (3), 325–346.
25. Ramesan, M.T. The effects of filler content on cure and mechanical properties of dichlorocarbene modified styrene butadiene rubber/carbon black composites. *J. Polymer Res.* **2004**, *11*, 333–340.
26. Pal, P.K.; De, S.K. Studies of polymer-filler interaction, network structure, physical properties and fracture of silica and clay-filled EPDM rubber in the presence of a silane coupling agent. *Rub. Chem. Tech.* **1983**, *56* (4), 737–773.